

The Role of Dynamo Fluctuations in Anomalous Ion Heating, Mode Locking, and Flow Generation

P. W. Terry 1), R. Gatto 1), R. Fitzpatrick 2), C.C. Hegna 3), and G. Fiksel 1)

1) Department of Physics, University of Wisconsin-Madison, Madison, WI 53706.

2) Institute for Fusion Studies, University of Texas at Austin, Austin, TX 78712.

3) Department of Engineering Physics, University of Wisconsin-Madison, Madison, WI 53706.

e-mail contact of main author: pwterry@facstaff.wisc.edu

Abstract. Anomalous ion heating intrinsic to magnetic fluctuation-induced electron heat transport, the locking of global modes through wall conditions, and flow generation via the magnetic Reynolds stress all derive from the global, $m=1$ tearing modes familiar in the RFP as the dynamo modes. These important processes are investigated analytically and numerically, yielding new insights and predictions for comparison with experiment.

1. Introduction

The large amplitude, $m=1$ global tearing modes unstable in the core of reversed field pinch (RFP) plasmas play a well-established role in the dynamo process that maintains toroidal field reversal. The amplitude and global extent of these modes also allows them to play a significant role in other important observed processes in the RFP. Three such processes are examined in this paper. The first is anomalous ion heating, manifested in the Ohmic equilibrium as an electron-ion temperature difference that is too small to be consistent with collisional equilibration, and in dramatic two-fold transient temperature increases during episodes of intense magnetic fluctuation activity associated with sawtooth events [1]. Sawtooth events, in particular, suggest that anomalous ion heating is intrinsic to magnetic turbulence, and the energy loss associated with electron motion along turbulent magnetic fields. The second process is the propensity for dynamo modes to form locked states involving error fields or eddy currents in resistive walls. The avoidance of locked modes, either through the reduction of error fields and a conducting boundary, or through plasma rotation, has been key to achieving optimal confinement. The third process is the creation of magnetic Reynolds stresses in sawtooth crashes, as observed in the Madison Symmetric Torus (MST). The magnetic Reynolds stress drives toroidal momentum, and hence a sheared $E \times B$ flow. The latter can diminish the intensity of both global magnetic modes and the more localized modes of the edge, both magnetic and electrostatic [2].

We find that 1) magnetic fluctuation-induced electron heat transport leads to ion heating through the observed process that slows the electron heat flux from the electron to the ion thermal velocity [3]. This accounts for both the observed ion temperature rise during sawtooth events, and a correlated decrease of electron temperature; 2) the threshold error field required for mode locking is reduced by the presence of a thin resistive vacuum vessel like that used in the Reversed Field Experiment (RFX); 3) the magnetic Reynolds stress during sawtooth events undergoes a large excursion from its nearly zero equilibrium value. The calculated radial eigenmode structure of edge tearing modes in the presence of a seed flow and strong pressure gradients suggests that these modes drive the observed Reynolds stress when their amplitudes are excited to a high level during a sawtooth crash by the nonlinear coupling to global modes.

2. Anomalous Ion Heating

Measurement of the field-aligned magnetic fluctuation-driven heat flux in MST is difficult to interpret in terms of conventional theory. Although there is an appreciable temperature gradient, the flux Q_e is convective. Moreover, if a Rechester-Rosenbluth expression is assumed, $Q_e = (\delta b/B_o)^2 l_{\parallel} v_t L_n^{-1} (nT)$, where L_n^{-1} is the density gradient scale length and l_{\parallel} is the parallel correlation length, it agrees with experiment only if the ion thermal velocity is used for v_t , and the fluctuation level $(\delta b/B_o)^2$ is that of the core-resonant tearing modes. If the fluctuation level of edge resonant modes is used (modes with $k_{\parallel}=0$ locally), the Rechester-Rosenbluth flux is too small even if v_t is the

electron thermal velocity [4]. However, the experimentally observed flux value agrees with a self-consistent theory of transport that accounts for the granular structures that form in the distribution of streaming electrons on scales below the magnetic fluctuation correlation. These structures, long hypothesized to occur in magnetic turbulence [5], behave like dressed test particles, but of macroscopic dimension. They are dressed with a dielectric shielding cloud that imposes a drag as they move along the field. The interaction with the cloud is governed by the collective mode response of the shielding charges. In the RFP this is dominated by the core-resonant tearing modes, even for the edge. The drag is mediated by the ions in the shielding cloud, slowing the rate at which electrons transport heat to the ion thermal velocity. Thus the theory reproduces the key features of the heat flux measurement.

A natural consequence of this process is the heating of ions as they absorb energy lost by the electrons due to the drag. In this mechanism, the heating source is the magnetic turbulence, and the heating rate H_i is tied to the electron heat flux Q_e . We present here the Kirchhoff's law that expresses the relationship between these two quantities, and then describe the results of a simple transport model for the evolution of the coupled electron and ion temperatures [6]. Consider the magnetic fluctuation-induced transport of parallel electron thermal energy. The magnetic part of the flux is $Q_e = -\int d^3v m_e v^2 v_{\parallel} (2B_o)^{-1} \langle \mathbf{b} \times \nabla A_{\parallel} \delta f_e \rangle$, where the electron distribution function δf_e satisfies a drift-kinetic equation. For simplicity we display only the parts proportional to the fluctuating magnetic vector potential A_{\parallel} , even though dependence on the electrostatic potential ϕ is retained in the calculation. The electron distribution has two components. One is the normal mode response of conventional theory and hence has a term proportional to each of the fluctuating potentials ϕ and A_{\parallel} ; the other is the granular component. A description of the latter requires solution of the two-point drift kinetic equation. It cannot be expressed as a response to either potential and cannot therefore be incorporated into the plasma dielectric. It remains in Ampere's law and the quasineutrality condition as a source. The normal mode and granular components are introduced into the flux, and quasineutrality and Ampere's law are imposed to account for the shielding of the granular component by the plasma dielectric. The resulting expression for the heat flux can be written, $Q_e^{\parallel} = -v_{it} D [L_{Ti}^{-1} + 2/3(1-\omega/\omega_{*i})L_{ni}^{-1}] n T_e$, where $D = 3/2\pi^{1/2} \Delta k_{\parallel}^{-1} (\delta b/B_o)^2 (v_{it}/v_{te})^2$ is a magnetic diffusivity and Δk_{\parallel} is the rms parallel wavenumber of the magnetic fluctuation spectrum [4]. The dependence on ion parameters reflects the slowing of electron granular structures by emission of energy into the shielding cloud, which damps on ions via Landau damping.

The parallel ion-heating rate is calculated from the correlation of the inductive electric field with the ion current fluctuation, $H_i = \langle E_{\parallel} J_{i\parallel} \rangle = -c^{-1} \langle (\partial A_{\parallel} / \partial t) J_{i\parallel} \rangle$. Because the ion current fluctuation enters Ampere's law, it can be expressed in terms of the electron contributions to Ampere's law. These are given by the current moment of the electron distribution δf_e , with the normal mode and granular components described above. As with the heat flux, the shielding of the granular component by the normal mode response is incorporated into the expression by imposing quasineutrality and Ampere's law. After some algebra we arrive at the expression

$$H_i = \sum_{\mathbf{k}, \omega} 2 \frac{|\Omega_e|}{\omega/k_{\parallel}} \frac{k_{\parallel}}{\mathbf{k} \times \mathbf{b}_o \cdot \mathbf{r}} Q_e^{\parallel}(\mathbf{k}, \omega),$$

where Ω_e is the electron gyrofrequency. This equation is the Kirchhoff's law that describes the relationship between ion heating and the ambipolar-constrained parallel electron heat loss. The underlying physical process is the absorption by ions of the energy lost by granular electron structures as they drag the dielectric shielding cloud. The energy exchange occurs via emission of radiation from moving test charges. Both the ion-heating rate and the flux of parallel electron heat are proportional to the magnetic fluctuation energy. If there is a rise in fluctuation activity the Kirchhoff's law predicts a rise in ion temperature correlated with a drop in electron temperature. Indeed, this is observed in Sawtooth crashes in MST. To assess if the magnitude of ion heating predicted by this expression is consistent with observations, the ion-heating rate is evaluated for parameters consistent with a sawtooth event in MST, and used in a simple 0-D transport model for ion and electron temperatures. This model includes collisional equilibration between ions and electrons, Ohmic heating of electrons, an anomalous loss rate in the ions, the ion-heating rate derived above, and electron loss rates due to the magnetic fluctuation-induced fluxes of electron

energy parallel and perpendicular to the field. The heat flux of parallel energy is given above. The flux of perpendicular energy has been calculated in Ref. [3]. In the core, the flux of perpendicular energy is not ambipolar-constrained and thus represents the dominant energy loss mechanism for electrons. The anomalous ion loss rate has not been calculated, but is estimated from the steady state balance prior to the sawtooth crash. This resulting rate is lower than experiment, giving a longer ion temperature decay time than that observed in experiment. Of interest here is whether the ion heating rate derived above is able to reproduce the magnitude of the ion temperature rise during a sawtooth crash. Integrating the heating rate over a crash time, the ion temperature is found to rise by amounts as large as several hundred eV, consistent with experimental observations. The time histories of ion and electron temperatures over a sawtooth crash as generated from this model are indicated in fig. 1. The heating rate depends on the fluctuation frequency, which has been taken from experiment. Variation of the frequency in a range bounded by the ion and electron diamagnetic frequencies shows that H_i is quite sensitive to frequency. It also is sensitive to the equilibrium profiles of temperature and density.

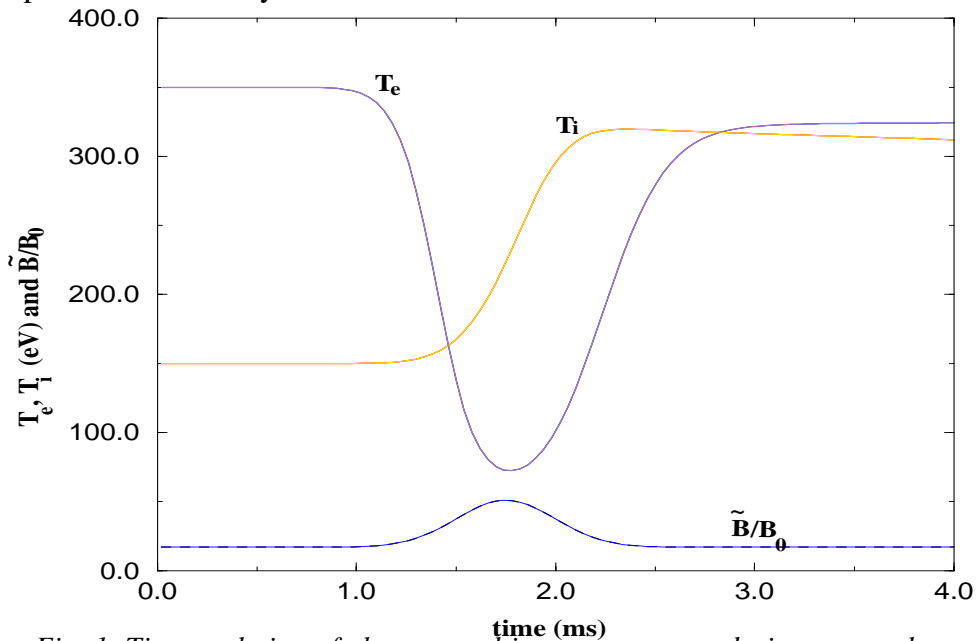


Fig. 1. Time evolution of electron and ion temperatures during sawtooth crash.

3. Locking of Dynamo Modes

The dominant MHD modes in the RFP are rotating, $m=1$ tearing modes, resonant in the plasma core. These dynamo modes are observed to *phase-lock* and form a toroidally localized structure in the perturbed magnetic field known as a slinky mode [7]. The slinky mode degrades plasma confinement primarily by channeling heat to produce a toroidally localized hot spot at the plasma edge. There is generally no problem as long as the slinky mode remains rotating. On the other hand, if the slinky mode stops rotating, the hot spot hovers over the same point on the plasma facing surface, causing overheating, impurity influx, and premature termination of the discharge. In the MST device, the slinky mode generally rotates, and there are no particular edge loading problems. In the RFX experiment it never rotates, and severe edge loading problems limit the maximum achievable plasma current. In the TPE-RX device, the slinky mode only rotates at very low plasma currents, and edge loading problems similar to those observed on RFX limit the maximum achievable plasma current.

There are two factors that could conceivably convert a slinky mode (and its constituent dynamo modes) from a rotating mode (which is its natural state) to a stationary mode. Firstly, static error-fields, which are generated primarily by the presence of insulating gaps in the thick conducting shell surrounding the plasma. The purpose of this shell, which is present in all RFPs, is the stabilization of dangerous external kink modes. Secondly, the resistive vacuum vessel, which in conventional RFPs (e.g., RFX, TPE-RX) is located between the plasma and the conducting shell. Eddy currents excited in this vessel can generate significant braking torques acting on rotating dynamo modes [8].

Error fields alone cannot account for the observed locked mode problems in RFX and TPE-RX. Admittedly, the error fields in RFX are slightly larger than those in MST. On the other hand, the error fields in TPE-RX are significantly smaller. Eddy currents excited in the resistive vacuum vessels of RFX and TPE-RX undoubtedly contribute to the locked mode problems. MST does not suffer from the same problem, since it does not possess a resistive vessel (the conducting shell plays the role of the vacuum vessel in this device). However, eddy currents alone cannot convert a rotating mode into a stationary one. Clearly, to account for the locked mode problems of present-day RFPs, we need to develop a comprehensive theory of rotation and locking of dynamo modes in the presence of both error fields and vacuum vessel eddy currents.

We have developed a set of phase evolution equations which govern the rotation and locking of a typical dynamo mode in the presence of both a resonant error-field and vacuum vessel eddy currents [9]. These equations are a generalization of the well-known equations of Zohm, *et al.* [10]. They *do not* assume the existence of a plasma region of fixed width that co-rotates with the mode. Instead, the extent of this region is determined self-consistently by plasma viscosity. From these equations we obtain thresholds for error-field locking, either in the absence or presence of the resistive shell. The locking threshold can be represented in the parameter space of normalized dynamo mode amplitude α_s and the normalized error-field amplitude α_c .

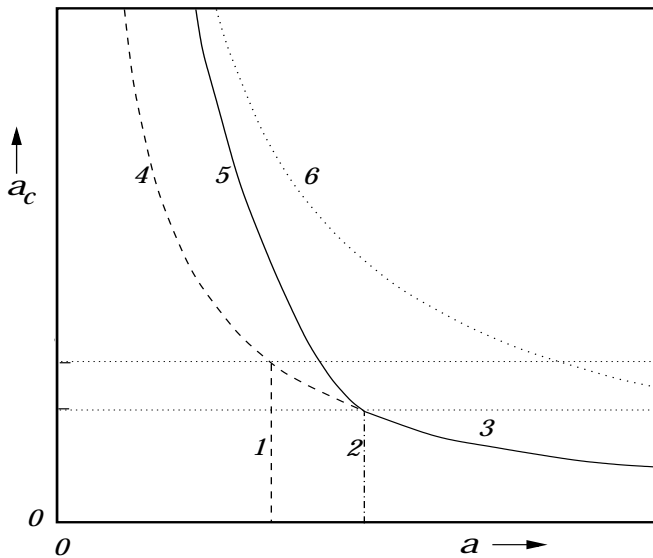


Fig. 2. Locking thresholds.

The curves labeled 3 and 5 in Fig. 2 represent the error-field locking threshold in the presence of a vacuum vessel. In the absence of a vacuum vessel the error-field locking threshold is given by the curve labeled 6. (The remaining curves represent thresholds for unlocking, or for the sudden slowing down or speeding up of mode rotation due to the braking torque exerted by the vacuum vessel eddy currents.) It is evident that error field locking occurs at lower dynamo mode amplitude and field error amplitude in the presence of a vacuum vessel. This indicates that the vacuum vessel strongly catalyzes locked mode formation. For RFX, we estimate that this effect reduces the error-field locking threshold by a factor of 5. It seems plausible, therefore, that the locked mode problems observed in RFX and TPE-RX are caused by a strong reduction in the error-field locking threshold due to the presence of a resistive vacuum vessel. This reduction renders otherwise innocuous error fields problematic.

4. Reynolds Stress Flow Shear Generation

The observed transient of the magnetic Reynolds stress from its nearly zero equilibrium value has been modeled by calculating the quasilinear Reynolds stress from edge resonant diamagnetic tearing modes in the presence of a seed shear flow. Treating the seed flow perturbatively, matched inner and outer layer equations are solved for $m=0$ (low n) and $m=1$ (high n) tearing modes. The

pressure gradient induces a diamagnetic frequency contribution to the tearing mode dispersion and an imaginary eigenmode component, allowing the Reynolds stress $R_M = (4\pi\rho_m)^{-1}\text{Re}\langle b_r b_\phi \rangle = (4\pi\rho_m)^{-1}\text{Im}\Sigma_n(n/R)\langle \psi \partial\psi/\partial r \rangle$ to become nonzero. The flow shear modifies the eigenmode structure and introduces an asymmetry in the radial gradient of the Reynolds stress that drives toroidal ion flow. Between sawtooth events, this nonzero Reynolds stress and its associated toroidal flow acceleration are weak because the modes that are localized in the edge where the pressure gradient is strong are typically only weakly excited. During a sawtooth event the fluctuation spectrum broadens and the edge resonant modes become strongly excited. The Reynolds stress tracks the burst of fluctuation activity associated with the sawtooth event, increasing first and then decaying to pre-sawtooth values as the spectrum relaxes. The radial localization of the Reynolds stress is determined by the radial eigenmode structure of the edge modes and the spectral energy distribution of cascaded energy, which maps via the q -profile to a spatial function. The importance of the $m=0$ mode in the cascade favors flow drive in proximity of the reversal layer, but $m=1$ modes localized away from the reversal layer also play a role. The mean toroidal flow is described by the toroidal ion momentum equation $\partial\langle V_{\phi,i} \rangle/\partial t = -\mu\langle V_{\phi,i} \rangle - (m_i R)^{-1}(\Gamma_{in} + \Gamma_{ex}) - \partial/\partial r[\langle v_{r,i} v_{\phi,i} \rangle - (4\pi\rho_m)^{-1}\langle b_r b_\phi \rangle]$. In this equation magnetic torques are represented by the Reynolds stress, which is dominated by edge resonant diamagnetic modes; by Γ_{ex} , which represents the interaction with external field errors as described above; and by Γ_{in} , which describes the internal torque exerted by core resonant global tearing modes. The latter attempts to force a three-wave resonant condition on the dominant interaction of two $m=1$ modes (with $n=6$ and $n=7$ for MST) and the $m=0, n=1$ mode, so that the plasma rotates as a rigid rotor at the phase velocity of the $m=0$ mode. In a sawtooth crash, the core modes are observed to decelerate first, with a subsequent slowing down at the edge induced by the internal torque. The Reynolds stress opposes the deceleration producing a localized flow shear. Measurements of $\partial\langle V_{\phi,i} \rangle/\partial t$ and the Reynolds stress indicate that the latter significantly exceeds the former, implying that the internal torque is also large and nearly in balance with the Reynolds stress.

Work supported by U.S.D.O.E.

- [1] SCIME, E., et al., "Ion heating and magnetohydrodynamic dynamo fluctuations in the reversed-field pinch", *Phys. Fluids B* **4**, (1992) 4062.
- [2] HEGNA, C.C., et al., "Theoretical studies of the role of flows and currents in the RFP", *Fusion Energy 1998 (Proc. 17th Int. Conf. Yolomama, 1998)*, IAEA, Vienna (1999) (CD-ROM file THP 1/10).
- [3] TERRY, P.W., et al., "Ambipolar magnetic fluctuation-induced heat transport in toroidal devices", *Phys. Plasmas* **3**, (1996) 1999.
- [4] SARFF, J., private communication.
- [5] TERRY, P.W., et al., "Self consistency constraints on turbulent magnetic transport and relaxation in a collisionless plasma", *Phys. Rev. Lett.* **57**, (1986) 1899.
- [6] GATTO, R., and TERRY, P.W., "Anomalous ion heating from ambipolar-constrained magnetic fluctuation induced transport in toroidal devices", *Phys. Plasmas*, submitted.
- [7] FITZPATRICK, R., "Formation and locking of the 'slinky mode' in reversed field pinches", *Phys. Plasmas* **6**, (1999) 1168.
- [8] FITZPATRICK, R., et al., "Effect of a resistive vacuum vessel on dynamo mode rotation in reversed field pinches", *Phys. Plasmas* **6**, (1999) 3878.
- [9] FITZPATRICK, R., and YU, E.P., "Nonlinear dynamo mode dynamics in reversed field pinches", *Phys. Plasmas* **7** (2000) 3610.
- [10] ZOHN, H., et al., "Plasma angular-momentum loss by MHD mode locking", *Europhys. Lett.* **11**, (1990) 745.